
Interpolation-based semi-supervised learning for object detection

Jisoo Jeong

Seoul National University
soo3553@snu.ac.kr

Vikas Verma

Aalto University, Finland,
Mila, Université de Montréal
vikas.verma@aalto.fi

Minsung Hyun

Seoul National University,
SK hynix
minsung.hyun@snu.ac.kr

Juho Kannala

Aalto University, Finland
juho.kannala@aalto.fi

Nojun Kwak *

Seoul National University
nojunk@snu.ac.kr

Abstract

Despite the data labeling cost for the object detection tasks being substantially more than that of the classification tasks, semi-supervised learning methods for object detection have not been studied much. In this paper, we propose an Interpolation-based Semi-supervised learning method for object Detection (ISD), which considers and solves the problems caused by applying conventional Interpolation Regularization (IR) directly to object detection. We divide the output of the model into two types according to the objectness scores of both original patches that are mixed in IR. Then, we apply semi-supervised learning methods suitable for each type. This method dramatically improves the performance of semi-supervised learning as well as supervised learning. In the semi-supervised learning setting, our algorithm improves the current state-of-the-art performance on benchmark dataset (PASCAL VOC07 as labeled data and PASCAL VOC12 as unlabeled data) and benchmark architectures (SSD300 and SSD512). In the supervised learning setting, our method, trained with VOC07 as labeled data, improves the baseline methods by a significant margin, as well as shows better performance than the model that is trained using the previous state-of-the-art semi-supervised learning method using VOC07 as the labeled data and VOC12 + MSCOCO as the unlabeled data. Code is available at: <https://github.com/soo89/ISD-SSD> .

1 Introduction

A dataset for object detection is much harder to create than the one for classification. While there is only one class in a single image for the classification task, there are multiple objects with different class labels in a single image for the object detection task. Therefore, the dataset for supervised object detection requires a pair of a class label and bounding box information for each object. Labeling each object takes more than a few seconds, and creating these datasets can take hundreds of hours [1, 2, 3].

Due to the higher time and resource complexity for creating object detection datasets, recently, methods for learning with weakly labeled data (D_W) or unlabeled data (D_U) have been studied as opposed to learning with only the labeled data (D_L)². There are mainly three types of this kind of object detection methods: weakly-supervised, semi-supervised, and weakly-semi-supervised learning.

*corresponding author

² $D_L = (I_i, y_i)_{i=1}^{N_L}$ where $y_i = (class^j, bbox^j)_{j=1}^{M_i}$, $D_W = (I_i, y_i)_{i=1}^{N_W}$ where $y_i = (class^j)_{j=1}^{M_i}$, and $D_U = (I_i)_{i=1}^{N_U}$. Here, N_X is the number of images, and M_i is the number of objects for the image I_i .

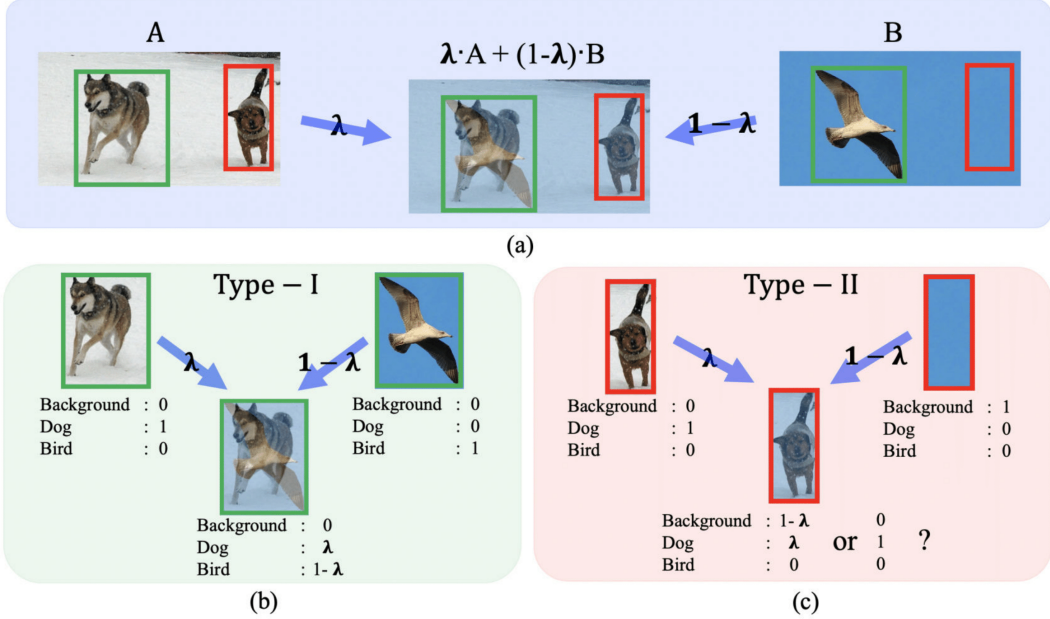


Figure 1: (a) mixed image created by random interpolation between images A and B (b) Type-I : both patches are from object classes. (c) Type-II : one of the patches is from the background class.

Weakly-supervised learning trains a model with a dataset that has only class information but no location information (D_W) [4, 5, 6, 7, 8]. On the other hand, weakly-semi-supervised learning is a learning method which uses D_W as well as D_L [9, 10]. Weakly-semi-supervised detector improves its performance compared to that of weakly-supervised learning, but it still needs to label classes for D_W . Instead of D_W , semi-supervised learning utilizes unlabeled data D_U as well as the labeled data (D_L) [11, 12, 13].

In this paper, we address the semi-supervised object detection problem and propose a new method called Interpolation-based Semi-supervised learning for object Detection (ISD) which can also be applied to the supervised learning framework. Interpolation Regularization (IR) which mixes different images and learns to predict the combined label rather than one hot vector performs outstandingly in supervised learning as well as in semi-supervised learning for classification problems [14, 15, 16, 17, 18]. However, it is challenging to apply IR directly to object detection because of the existence of the background class that has very diverse and irregular texture. Fig. 1 shows an example. In Fig. 1(a), we mix image A and B using the mixing parameter $\lambda = 0.5$ as shown in the middle. Obviously, the mixed green box has 0.5 of dog and 0.5 of bird as can be seen in Fig. 1(b). However, when an object is mixed with a background as can be seen in Fig. 1(c), the mixed image appears to be a 100% object corrupted by noise. If the detector is trained by the conventional IR, any blurred or noisy mixture images contribute to increasing the confidence of the background class, and it will degrade performance.

To tackle this problem, in this paper, we divide the mixed images into two types (Type-I and II) considering whether one of the original image is the background or not. Then, we apply a different IR algorithm suitable for each type. The proposed ISD method which will be detailed in Sec. 3 can be combined with conventional semi-supervised learning methods such as CSD (consistency-based semi-supervised learning) [13] to produce state-of-the-art semi-supervised object detection performances. Also, the proposed scheme can be used to enhance the detection performance in the supervised learning framework. Our main contributions can be summarized as follows:

- We show the problem in applying interpolation regularization directly to the object detection task and propose a novel interpolation-based semi-supervised learning algorithm for object detection.
- In doing so, we define two types of interpolation cases in the object detection task and propose efficient semi-supervised learning methods suitable for each type.

- We experimentally show the effectiveness of the proposed method for each type by demonstrating a significant performance improvement over the conventional algorithms achieving SOTA semi-supervised object detection performance.
- The proposed method can also be applied to the framework of supervised learning, improving the detection performance significantly.

2 Related Work

Interpolation-based regularization is a promising approach due to its state-of-the-art performances and virtually no additional computational cost. These methods construct additional training samples by combining two or more training samples. Mixup [14] and Between-class learning [19] are the earliest works that took steps in this direction. These methods are based on the principle that the output of a supervised network for an affine combination of two training samples should change linearly. Such kind of inductive bias can be induced in a network by training it on the synthetic samples constructed by *mixing* two samples and their corresponding targets. Manifold Mixup [15] mixes features in the deeper layers instead of input images. Other works such as CutMix [20] construct the synthetic samples by mixing the CutOut [21] versions of two samples. Overall, these approaches can be interpreted as a form of data-augmentation technique that seeks to construct additional training samples by combining two or more samples. In the unsupervised learning setting, interpolation-based regularizers have been explored in ACAI [22] and AMR [23]. These methods learn better unsupervised representations by enforcing a constraint that the representations obtained by mixing the representations of two samples should correspond to a data point on the data manifold.

Semi-supervised learning (SSL) is a dominant approach for machine learning when the annotated data is scarce. There has been recent surge of interest in deep learning based on SSL for object classification [16, 17, 18]. These methods can be broadly categorized into: (1) consistency regularization methods (2) generative adversarial networks (GAN) based methods. Consistency regularization methods are more appealing due to their simplicity, training stability and state-of-the-art performance.

The central idea of the consistency regularization methods is to enforce that the model predictions should not change under *reasonable* permutations to the input. For object classification, such permutations entail random translation, random cropping and horizontal flipping etc. Let us assume that x and x' are the original and the permuted inputs, $d(\cdot, \cdot)$ be a distance function, $w(t)$ be a weighting function over iterations t and $f(\cdot)$ be a function on which consistency loss is measured, then the consistency loss L_U is computed in an unsupervised manner and consequently the total loss L_{total} is given by a linear combination of the consistency loss and the supervised loss L_S as follows:

$$L_U = d(f(x), f(x')), \quad L_{total} = L_S + w(t) \cdot L_U. \quad (1)$$

Some notable examples of consistency training include PI model [24], virtual adversarial training [25] and Mean Teacher [26]. The recent advances in this direction includes interpolation consistency training (ICT) [16] (its variants MixMatch [17], ReMixMatch [27] and FixMatch [28]).

ICT is a specific type of consistency regularization that encourages the prediction at an interpolation of unlabeled samples to be consistent with the interpolation of the predictions at those samples. FixMatch uses another form of consistency regularization, where the model’s prediction on “weak augmentation” are encouraged to be consistent with the “strong augmentation”. For weak augmentation, FixMatch uses horizontal flipping, random translation and cropping, and for strong augmentation it uses Cutout [21], RandAugment[29] and CTAugment[27].

Semi-supervised learning for object detection has recently been studied in [13] where CSD, the first consistency-regularization-based semi-supervised object detection method, was proposed. They explored the consistency between the box predictions in the original and the horizontally flipped version. To prevent the ‘background’ class from dominating the consistency loss in Eq. (1), they proposed the Background Elimination (BE) method which excludes boxes with high background probability in the computation of the consistency loss. In this paper, we also utilize the BE using the class probability of each candidate box.

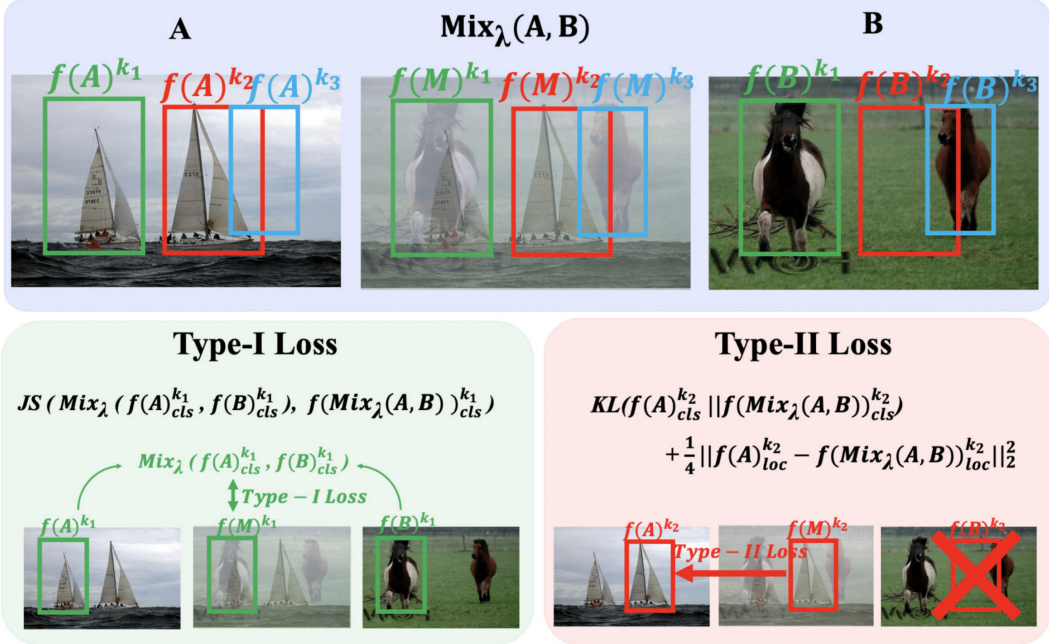


Figure 2: The proposed ISD loss for each type. $Mix_\lambda(a, b) = \lambda \cdot a + (1 - \lambda) \cdot b$

3 Method

We denote a horizontally flipped version of an image A as \hat{A} , and the image created by random mixing $\lambda \cdot A + (1 - \lambda) \cdot B$ between two images A and B as $Mix_\lambda(A, B)$. Similar to Mixup, the mixing coefficient λ is drawn from the $Beta(\alpha, \alpha)$ distribution. In our method, we use SSD [30], one of the most popular single-stage object detectors, as a detector. In the training of SSD, we add the newly proposed interpolation-based consistency regularization loss in combination with the flip-based consistency regularization loss in [13] to enhance the performance. The network output of SSD $f^{p,r,c,d}$ is denoted as the output of the p^{th} layer of the pyramid, r^{th} row, c^{th} column and d^{th} default box, and (p, r, c, d) is expressed as k for brevity. Each f^k is composed of f_{cls}^k and f_{loc}^k which are the softmax output vector and the localization offsets of the center and the size of the box, $[\Delta cx, \Delta cy, \Delta w, \Delta h]$, at position k , respectively. The mask $m(I)$, which is computed by $f_{cls}(I)$, is used in background elimination and interpolation type categorization for image I and has the binary objectness value at each location k :

$$m(I)^k = \begin{cases} 1, & \text{if } \text{argmax}(f_{cls}^k(I)) \neq \text{background} \\ 0, & \text{otherwise.} \end{cases} \quad (2)$$

3.1 Interpolation-based Semi-supervised learning for Object Detection (ISD)

Type categorization. We determine the type of a pair of patches by the background elimination method [13] that only extracts patches with a high objectness probability. Then we apply different methods appropriate for each type of patches. Eq. (3) is how we calculate each type of a mask. The Type-I mask, m_I , is calculated by element-wise multiplication of $m(A)$ and $m(B)$. In other words, it becomes 1 when both patches of $m(A)^k$ and $m(B)^k$ are 1, and otherwise it is 0. On the other hand, the Type-II mask m_{II}^A (m_{II}^B) is calculated by element-wise multiplication of $m(A)(m(B))$ and $\sim m(B)(\sim m(A))$, which means it is 1 when the patch in image $A(B)$ has a high objectness score while the corresponding patch at the same location in image $B(A)$ has a high background score.

$$m_I = m(A) \otimes m(B), \quad m_{II}^A = m(A) \otimes \sim m(B), \quad m_{II}^B = \sim m(A) \otimes m(B). \quad (3)$$

Type I loss: When the patches in the image A and B are all likely to be objects (Type-I), we define a Type-I loss inspired by the ICT loss [16]. Note that there are two differences compared to conventional

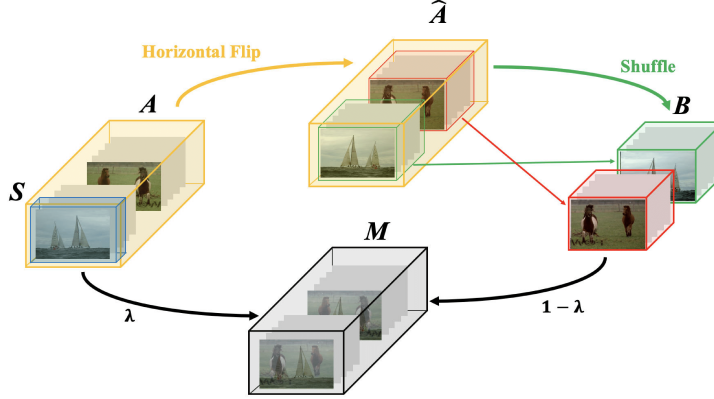


Figure 3: Combination of ISD with CSD. The original images (\mathcal{A}) are flipped ($\hat{\mathcal{A}}$) and the mixed images (\mathcal{M}) are obtained by combining the two. First, the order of flipped images are changed by shuffling ($\mathcal{B} = \text{shuffle}(\hat{\mathcal{A}})$), then \mathcal{A} and \mathcal{B} are mixed ($\mathcal{M} = \text{Mix}_\lambda(\mathcal{A}, \mathcal{B})$). CSD loss is calculated between \mathcal{A} and $\hat{\mathcal{A}}$ and ISD loss is computed between \mathcal{M} and (\mathcal{A} and/or \mathcal{B}). In the original set (\mathcal{A}), the blue box (\mathcal{S}) is labeled, to which the supervised loss is applied.

ICT. First, we used *Jensen-Shannon divergence* (JSD) as the consistency regularization loss (function $d(\cdot, \cdot)$ in Eq. (1)). Second, we use the same network to feed-forward inputs like CSD, distinct from ICT which uses different networks for mixed and original inputs using MeanTeacher [26]. Eq. (4) shows the loss function of Type-I, which is the distance between the mixed output of $f(A)_{cls}^k$ and $f(B)_{cls}^k$ and the output of the mixed image of A and B , $f(\text{Mix}_\lambda(A, B))_{cls}^k$.

$$l_I = JS(f(A)_{cls}^k, f(B)_{cls}^k) \| f(\text{Mix}_\lambda(A, B))_{cls}^k \quad (4)$$

The overall Type-I loss \mathcal{L}_I is the average of patches whose Type-I mask is 1, i.e. $\mathcal{L}_I = \mathbb{E}_{\mathbb{I}\{m_I=1\}}[l_I]$. Here, \mathbb{E} and \mathbb{I} are the expectation and the indicator function, respectively.

Type II loss: As shown in Fig. 2, in Type II, one patch has a high probability of foreground, while the other has a high probability of background. In this case, instead of using the Type I loss described above, we train the network to have similar predictions on the mixed patch and the patch with high probability of foreground. This kind of loss can be interpreted as a form of FixMatch loss [28] which encourages consistency between the predictions on the strong augmentation and the weak augmentation of an input. This parallel can be seen by considering the mixed patch as a strong augmentation and patch with high foreground probability as no-augmentation. Note that, for classification, FixMatch is trained with targets by creating pseudo-labeling of samples that exceed the threshold, whereas we do not need to set a specific threshold and the target is set to the output distribution of no-augmentation patch.

We set $f(A)$ or $f(B)$ as a target, and train the mixed output ($f(\text{Mix}_\lambda(A, B))$) to be close to $f(A)$ or $f(B)$. In doing so, Kullback-Leibler (KL) divergence and L2 loss are used as the classification and localization losses, respectively as follows:

$$l_{II_cls}^A = KL(f(A)_{cls}^k \| f(\text{Mix}_\lambda(A, B))_{cls}^k), \quad l_{II_loc}^A = \frac{1}{4} \| f(A)_{loc}^k - f(\text{Mix}_\lambda(A, B))_{loc}^k \|_2^2. \quad (5)$$

The overall Type-II loss when patch A is foreground, \mathcal{L}_{II}^A , is calculated as the average of the sum of two individual losses as $\mathcal{L}_{II}^A = \mathbb{E}_{\mathbb{I}\{m_{II}^A=1\}}[l_{II_cls}^A + l_{II_loc}^A]$. Likewise, \mathcal{L}_{II}^B is also calculated by applying the above loss, and the total loss of Type-II is calculated as $\mathcal{L}_{II} = \mathcal{L}_{II}^A + \mathcal{L}_{II}^B$.

Finally, the overall ISD loss is computed by Type-I loss (\mathcal{L}_I) and Type-II loss (\mathcal{L}_{II}) as follows:

$$\mathcal{L}_{ISD} = \gamma_1 \cdot \mathcal{L}_I + \gamma_2 \cdot \mathcal{L}_{II}. \quad (6)$$

Table 1: Detection results for PASCAL VOC2007 test set under the supervised training setting.

Method	Labeled Data	Backbone Network	mAP (%)	Speed (FPS)
SSD300 [30, 13]	VOC07	VGG16	70.2	$\times 1$
SSD300 (CSD) [13]	VOC07	VGG16	69.3	
SSD300 (ISD)	VOC07	VGG16	72.63 \pm 0.67	
SSD300 (ISD + CSD)	VOC07	VGG16	72.73 \pm 0.12	
SSD300 [30, 13]	VOC07 + VOC12	VGG16	77.2	$\times 1$
SSD300 (ISD + CSD)	VOC07 + VOC12	VGG16	78.60 \pm 0.10	
RSSD300 [33]	VOC07 + VOC12	VGG16	78.5	
DSSD321 [34]	VOC07 + VOC12	ResNet-101	78.6	
SSD512 [30, 13]	VOC07 + VOC12	VGG16	79.6	$\times 1$
SSD512 (ISD + CSD)	VOC07 + VOC12	VGG16	81.17 \pm 0.15	
RSSD512 [33]	VOC07 + VOC12	VGG16	80.8	
DSSD513 [34]	VOC07 + VOC12	ResNet-101	81.5	

Table 2: Detection results for PASCAL VOC2007 test set under the semi-supervised training setting. The following experiments use VOC07 (labeled) and VOC12 (unlabeled) data. **Blue** and **Red** are represented as the Baseline score and Best score, respectively.

SSL Algorithm	Labeled data	Unlabeled data	mAP (%)	
			SSD 300	SSD 512
Supervised Learning [30, 13]	VOC07	-	70.2	73.3
	VOC07 + VOC12	-	77.2	79.6
CSD [13]	VOC07	VOC12	72.3	75.8
Ours (ISD only)	VOC07	VOC12	73.27 \pm 0.50	76.37 \pm 0.45
Ours (ISD + CSD)	VOC07	VOC12	74.20 \pm 0.10	76.77 \pm 0.06

3.2 Combination of ISD with CSD

For ISD training, three sets of image batches, \mathcal{A} , \mathcal{B} , and $\mathcal{M} = Mix_{\lambda}(\mathcal{A}, \mathcal{B})$ should be inferred by the network. For efficient training, we set the batches \mathcal{A} and $\hat{\mathcal{A}}$ as the original images and their horizontally flipped versions as shown in Fig. 3, between which the CSD loss is applied. However, if an image $A \in \mathcal{A}$ and its horizontal flipped version $\hat{A} \in \hat{\mathcal{A}}$ are mixed, the mixed image $Mix_{\lambda}(A, \hat{A})$ would have similar backgrounds and will have the same class in the center of the image. Therefore, as shown in Fig. 3, we make the mixed images by combining the original batch (\mathcal{A}) with the half-shuffled flipped batch ($\mathcal{B} = \text{shuffle}(\hat{\mathcal{A}})$). The total loss consists of supervised loss (\mathcal{L}_S), CSD loss (\mathcal{L}_{CSD}), and ISD loss (\mathcal{L}_{ISD}) as follows:

$$\mathcal{L}_{Total} = \mathcal{L}_S + w(t) \cdot [\mathcal{L}_{CSD} + \mathcal{L}_{ISD}], \quad (7)$$

where $w(t)$ is a weight scheduling function.

4 Experiments

We set up the experiment in the same environment as that of the conventional semi-supervised learning methods for object detection. Similar to [11, 13], we trained our model with PASCAL VOC07 *trainval* (5k images) dataset [31] as labeled data and PASCAL VOC12 *trainval* (12k images) & MSCOCO *trainval* (123k images) dataset [32] as unlabeled data and tested with PASCAL VOC07 test dataset. PASCAL VOC and MS COCO data consist of 20 and 80 classes, respectively. For the unlabeled MSCOCO dataset, we experiment with MSCOCO (full) and MSCOCO (VOC) that consists of only VOC classes in each image as in [13]. We sample the mixing parameter λ from Beta(α, α) at every iteration. The parameters are set to $\{\gamma_1, \gamma_2\} = \{0.1, 1\}$ in eq. (6) and $\alpha = 5$ in beta distribution. Since the number of samples of Type-I is less than the number of samples of Type-II, we set γ_1 as 0.1 to reduce the weight in each sample in Type-I. Other learning parameters such as learning rate and batch size are the same as [13]. In our experiment, we report the mean and standard deviation of the results of three runs.

Table 3: Detection results for PASCAL VOC2007 test set. The following experiments use VOC07 (labeled) and VOC12 & MSCOCO (unlabeled) data.

Detector	Labeled data	Unlabeled data	mAP (%)	
			CSD [13]	Ours (ISD + CSD)
SSD300	VOC07	VOC12	72.3	74.20 \pm 0.10
		VOC12 + MSCOCO (full)	71.7	73.57 \pm 0.15
		VOC12 + MSCOCO(VOC)	72.6	74.40 \pm 0.10

4.1 Supervised Learning

We start by examining the effect of ISD on SSD300 in the supervised training setting. The results are presented in Table 1. In the first row block, SSD300 (base) trained with VOC 07 (*trainval*) data shows 70.2 mAP performance, while that of SSD300 (CSD) decreases to 69.3 mAP, which shows a clear side effect of over-regularization. On the other hand, SSD300 (ISD) and SSD300 (ISD + CSD) show 2.43% and 2.53% improvements in accuracy compared to SSD300 (base), respectively. Note also that the standard deviation of ISD+CSD is quite lower than that of ISD only. This shows that combining ISD with a strong CSD regularizer stabilizes the training, making the network more robust to random batches and random choice of mixing parameter λ .

In the second and the third row blocks of Table 1, SSD300 (base) and SSD512 (base) trained with VOC 07+VOC12 (*trainval*) data show 77.2% and 79.6%, respectively. SSD300 (ISD+CSD) shows 1.4% of enhancement and SSD512 (ISD+CSD) shows 1.5% of enhancement. We compared our algorithm to those of other SSDs with similar losses and a few different structures. RSSD [33] and DSSD [34] are models that efficiently change the feature pyramid to improve the performance of SSD, but at the cost of degraded training and inference speed.³ The SSD300 (ISD + CSD) model shows a performance improvement close to the RSSD300 and DSSD321 without changing the network structure, and the SSD512 (ISD + CSD) model shows better performance than the RSSD512. SSD512 equipped with our ISD+CSD in the training stage achieves comparable performance to that of DSSD (less than 0.5% difference). This is particularly appealing because at inference time, DSSD513 is about 3 to 5 times slower than SSD. Interestingly, ISD training of SSD300 in a fully supervised manner using just the VOC07 dataset outperforms previous state-of-the-art semi-supervised learning method (CSD) that use VOC07 as labeled data as well as VOC12 as unlabeled data (compare row 3 of Table 1 and row 1 of Table 3).

4.2 Semi-Supervised Learning

We evaluate the performance of ISD in the SSL setting. As shown in Table 2, the performance of the SSD300 model trained only with VOC07 labeled data is 70.2%. The performance of SSD300 model with VOC07 labeled data and VOC12 unlabeled data for CSD (previous state-of-the-art method), ISD and ISD+CSD is 72.3%, 73.27%, and 74.20% respectively. This demonstrates the effectiveness of our approach in SSL setting. Moreover, ISD+CSD with VOC07 labeled data and VOC12 unlabeled data on SSD300 (Table 2, last row) shows 1.47% performance improvement in comparison to the fully supervised setting with VOC07 labeled data on SSD300 (Table 1, row 4). This demonstrates that the performance gain is not due to ISD+CSD applied only on the labeled data; unsupervised versions of ISD+CSD loss are crucial for better performance. Similar to SSD300, for SSD512, ISD shows significant improvement over CSD, with ISD + CSD achieving the best performance. We further extend the experimental analysis by using the MSCOCO dataset in addition to the VOC12 dataset as the unlabeled samples. The results shown in Table 3 demonstrate that across all the unlabeled datasets, our ISD+CSD approach outperforms baseline CSD-only approach by a significant margin.

5 Discussion

Ablation studies for Type-I and Type-II : We experiment to verify the performance of each type, and each column in Table 4 represents the different types of ISD methods. We added each type of ISD loss on the CSD baseline, which reduces standard deviation of the experimental result. When

³Since the GPU type, implementation, and criterion of speed measurement are all different for each literature, we show the speed in each paper as a relative ratio of speed drop compared to that of SSD.

Table 4: Ablation study for α and each type in VOC07(L) + VOC12(U) training dataset and VOC07 testing dataset. The row represents the α of the beta distribution, and the column represents each type. All the experiments in this table are performed by adding each loss to the CSD. (CSD-only performed 72.3%).

$\beta(\alpha, \alpha)$	SSD300 + ISD Method (mAP (%))		
	Type-I	Type-II	Type-I + Type-II
1	72.07 ± 0.32	72.97 ± 0.06	73.40 ± 0.36
2	72.57 ± 0.15	73.80 ± 0.26	73.87 ± 0.15
5	72.47 ± 0.21	74.07 ± 0.15	74.20 ± 0.10
10	72.00 ± 0.40	73.37 ± 1.01	73.87 ± 0.55

Table 5: Ablation study of Type-II losses on PASCAL VOC2007 test set. All the experiments in this table are performed by adding each loss to the CSD. (α is 5 and CSD-only performed 72.3%).

VOC07(L)+VOC12(U)	mAP (%)
Type-II (cls)	73.70 ± 0.20
Type-II (loc)	73.17 ± 0.15
Type-II (cls + loc)	74.07 ± 0.15

we apply Type-I loss, there is a little improvement from CSD (72.3%) where α is 2. On the other hand, when type-II loss is applied, the performance increases significantly compared to Type-I and increases most when α is 5. There are three reasons for the above results. First, the numbers of Type-I and Type-II samples are different. With a trained model, the number of Type-II samples were 5 times that of Type-I samples, which indicates that the influence of Type-I loss is relatively small. Second, Type-I only considers the classification loss. While the boundaries of the two object that created the mixed patch are in different locations, the boundary of the mixed patch is not interpolated. Therefore, the localization loss cannot be applied in Type-I. Third, two objects that are mixed may not be aligned well. More research is needed for the alignment in Interpolation Regularization, which remains as a future work. Finally, combining Type-I and Type-II improves the performance on all α values.

In Table 5, we analyzed the effect of the classification and the localization loss in Type-II when α is 5. The classification loss on Type-II samples showed more remarkable performance improvement than the localization loss, and by combining them, we can obtain better performance.

Beta distribution : In ISD, the mixing coefficient λ is sampled from the $Beta(\alpha, \alpha)$ distribution. Table 4 shows the performance of ISD using various values of α across different types of ISD losses. We observe that a large range of α gives improved performance in comparison to the baseline (CSD with 72.3% mAP), showing that ISD is not very sensitive to the value of α . In general, we recommend to set α to a sufficiently large value such as in the range of [2,5]. The reason for choosing relatively large α is as follows: With a smaller values of α (e.g. $\alpha < 1$), λ will be close to either 0 or 1 with high probability, thus most of the mixed images will be closer to either of the original images being mixed. In this case, the mixed image M will be extremely weak (for one image) or strong (for the other) augmentation resulting in lowered performance with high variance. In contrast, increasing the values of α increases the probability of λ being closer to 0.5, which provides an appropriate level of regularization. Note that if the value of α is too large, λ will be concentrated too much around 0.5 (e.g. for $\alpha = 10$, $Pr(0.2 \leq \lambda \leq 0.8) = 0.997$) and all the augmented samples will be too different from the original images resulting in degraded performance with high variance at test time.

Training model size : For ISD training, image batches are inferred by the network three times over conventional SSD. Also, due to the calculation of additional losses, it requires more than three times the conventional SSD memory. We used Nvidia 1080Ti GPU, and we assigned 4 and 8 GPUs for SSD300 and SSD512 models with ISD training, respectively. With fewer GPUs, our implementation was not trainable because of limited memory budget. However, at testing, it has the same network size and inference time as the base network and can improve the performance.

Object detector : In this paper, we have used the SSD model among single stage detectors. In the case of other detectors, algorithm-specific modifications should be made to successfully apply interpolation regularization. However, the basic idea of separating Type-I and Type-II samples and applying different loss for each case can still be valid. In the case of a Two-Stage detector, for example, Region of Interest (RoI) is obtained by Region Proposal Network (RPN) and classification of that location is performed for object detection. Since the RoIs of A , \hat{A} , B , and $Mix_\lambda(A, B)$ are all different, in order to apply our algorithm, one of RoIs should be applied to other images for one-to-one correspondence. If the RoI of A is applied to other images, Type-II loss between B and $Mix_\lambda(A, B)$ cannot be obtained, and if each RoI of A , B , $Mix_\lambda(A, B)$ is applied individually to

other images, a lot of computation will be required. Thus how to apply interpolation-based regularizer for Two-stage detectors is an interesting avenue for research.

6 Conclusion

In this paper, we have proposed ISD, a simple and efficient Interpolation-based semi-supervised learning algorithm for object detection using single-stage detectors. We started by investigating the challenges that occur when the Interpolation Regularization methods for the classification task are applied directly to an object detection task, and have addressed these challenges by proposing different types of interpolation-based loss functions. Our method shows significant improvement in both semi-supervised and supervised object detection tasks over the previous state-of-the-art methods, compared over the same dataset and the same architecture settings. We further demonstrate that combining ISD with the previous method of CSD can further improve the performance and advance the current state-of-the-art. We leave the exploration of Interpolation Regularization for Two-stage detectors as a future work.

7 Statement of the potential broader impact of this work

ISD is a fundamental algorithm for object detection in images, which could conceivably used for any application that requires object detection. It allows for training with unlabeled data, which may make it more useful for those with only a small amount of labeled data and make it more widely usable, and may facilitate new applications of object detection. For example, extending ISD to the medical vision application can be particularly useful, since the labeled data is usually scarce in these domains. Furthermore, it might make smaller organizations or non-profits which have less budget for collecting labeled data more competitive with larger organizations. In general, improving performance for the object detection task could have a variety of applications, which could be positive, negative, or more complicated, but would depend on the nature of the organization using them and what task they use them for.

References

- [1] Olga Russakovsky, Li-Jia Li, and Li Fei-Fei. Best of both worlds: human-machine collaboration for object annotation. In *Proceedings of the IEEE conference on computer vision and pattern recognition*, pages 2121–2131, 2015.
- [2] Amy Bearman, Olga Russakovsky, Vittorio Ferrari, and Li Fei-Fei. What’s the point: Semantic segmentation with point supervision. In *European conference on computer vision*, pages 549–565. Springer, 2016.
- [3] Piotr Dollar, Christian Wojek, Bernt Schiele, and Pietro Perona. Pedestrian detection: An evaluation of the state of the art. *IEEE transactions on pattern analysis and machine intelligence*, 34(4):743–761, 2012.
- [4] Yi Zhu, Yanzhao Zhou, Qixiang Ye, Qiang Qiu, and Jianbin Jiao. Soft proposal networks for weakly supervised object localization. In *Proceedings of the IEEE International Conference on Computer Vision*, pages 1841–1850, 2017.
- [5] Miaojing Shi, Holger Caesar, and Vittorio Ferrari. Weakly supervised object localization using things and stuff transfer. In *Proceedings of the IEEE International Conference on Computer Vision*, pages 3381–3390, 2017.
- [6] Zequn Jie, Yunchao Wei, Xiaojie Jin, Jiashi Feng, and Wei Liu. Deep self-taught learning for weakly supervised object localization. In *Proceedings of the IEEE Conference on Computer Vision and Pattern Recognition*, pages 1377–1385, 2017.
- [7] Jiajie Wang, Jiangchao Yao, Ya Zhang, and Rui Zhang. Collaborative learning for weakly supervised object detection. *arXiv preprint arXiv:1802.03531*, 2018.
- [8] Daesik Kim, Gyujeong Lee, Jisoo Jeong, and Nojun Kwak. Tell me what they’re holding: Weakly-supervised object detection with transferable knowledge from human-object interaction. *arXiv preprint arXiv:1911.08141*, 2019.

- [9] Yuxing Tang, Josiah Wang, Boyang Gao, Emmanuel Dellandréa, Robert Gaizauskas, and Liming Chen. Large scale semi-supervised object detection using visual and semantic knowledge transfer. In *Proceedings of the IEEE Conference on Computer Vision and Pattern Recognition*, pages 2119–2128, 2016.
- [10] Ziang Yan, Jian Liang, Weishen Pan, Jin Li, and Changshui Zhang. Weakly-and semi-supervised object detection with expectation-maximization algorithm. *arXiv preprint arXiv:1702.08740*, 2017.
- [11] Keze Wang, Xiaopeng Yan, Dongyu Zhang, Lei Zhang, and Liang Lin. Towards human-machine cooperation: Self-supervised sample mining for object detection. In *Proceedings of the IEEE Conference on Computer Vision and Pattern Recognition*, pages 1605–1613, 2018.
- [12] Nhu-Van Nguyen, Christophe Rigaud, and Jean-Christophe Burie. Semi-supervised object detection with unlabeled data. In *international conference on computer vision theory and applications*, 2019.
- [13] Jisoo Jeong, Seungeui Lee, Jeesoo Kim, and Nojun Kwak. Consistency-based semi-supervised learning for object detection. In *Advances in Neural Information Processing Systems*, pages 10758–10767, 2019.
- [14] Hongyi Zhang, Moustapha Cisse, Yann N. Dauphin, and David Lopez-Paz. mixup: Beyond empirical risk minimization. In *International Conference on Learning Representations*, 2018.
- [15] Vikas Verma, Alex Lamb, Christopher Beckham, Amir Najafi, Ioannis Mitliagkas, David Lopez-Paz, and Yoshua Bengio. Manifold mixup: Better representations by interpolating hidden states. In Kamalika Chaudhuri and Ruslan Salakhutdinov, editors, *Proceedings of the 36th International Conference on Machine Learning*, volume 97 of *Proceedings of Machine Learning Research*, pages 6438–6447, Long Beach, California, USA, 09–15 Jun 2019. PMLR.
- [16] Vikas Verma, Alex Lamb, Juho Kannala, Yoshua Bengio, and David Lopez-Paz. Interpolation consistency training for semi-supervised learning. In *Proceedings of the Twenty-Eighth International Joint Conference on Artificial Intelligence, IJCAI-19*, pages 3635–3641. International Joint Conferences on Artificial Intelligence Organization, 7 2019.
- [17] David Berthelot, Nicholas Carlini, Ian Goodfellow, Nicolas Papernot, Avital Oliver, and Colin A Raffel. Mixmatch: A holistic approach to semi-supervised learning. In *Advances in Neural Information Processing Systems*, pages 5050–5060, 2019.
- [18] Vikas Verma, Meng Qu, Alex Lamb, Yoshua Bengio, Juho Kannala, and Jian Tang. Graphmix: Regularized training of graph neural networks for semi-supervised learning. *ArXiv*, abs/1909.11715, 2019.
- [19] Yuji Tokozume, Yoshitaka Ushiku, and Tatsuya Harada. Between-class learning for image classification. In *The IEEE Conference on Computer Vision and Pattern Recognition (CVPR)*, June 2018.
- [20] Sangdoo Yun, Dongyoon Han, Seong Joon Oh, Sanghyuk Chun, Junsuk Choe, and Youngjoon Yoo. Cutmix: Regularization strategy to train strong classifiers with localizable features. *arXiv preprint arXiv:1905.04899*, 2019.
- [21] Terrance Devries and Graham W. Taylor. Improved regularization of convolutional neural networks with cutout. *CoRR*, abs/1708.04552, 2017.
- [22] David Berthelot, Colin Raffel, Aurko Roy, and Ian Goodfellow. Understanding and improving interpolation in autoencoders via an adversarial regularizer. In *International Conference on Learning Representations*, 2019.
- [23] Christopher Beckham, Sina Honari, Vikas Verma, Alex M Lamb, Farnoosh Ghadiri, R Devon Hjelm, Yoshua Bengio, and Chris Pal. On adversarial mixup resynthesis. In *Advances in Neural Information Processing Systems*, pages 4348–4359, 2019.
- [24] Samuli Laine and Timo Aila. Temporal ensembling for semi-supervised learning. *arXiv preprint arXiv:1610.02242*, 2016.
- [25] Takeru Miyato, Shin-ichi Maeda, Shin Ishii, and Masanori Koyama. Virtual adversarial training: a regularization method for supervised and semi-supervised learning. *IEEE transactions on pattern analysis and machine intelligence*, 2018.

- [26] Antti Tarvainen and Harri Valpola. Mean teachers are better role models: Weight-averaged consistency targets improve semi-supervised deep learning results. In *Advances in neural information processing systems*, pages 1195–1204, 2017.
- [27] David Berthelot, Nicholas Carlini, Ekin D. Cubuk, Alex Kurakin, Kihyuk Sohn, Han Zhang, and Colin Raffel. Remixmatch: Semi-supervised learning with distribution matching and augmentation anchoring. In *International Conference on Learning Representations*, 2020.
- [28] Kihyuk Sohn, David Berthelot, Chun-Liang Li, Zizhao Zhang, Nicholas Carlini, Ekin D. Cubuk, Alex Kurakin, Han Zhang, and Colin Raffel. Fixmatch: Simplifying semi-supervised learning with consistency and confidence. *arXiv preprint arXiv:2001.07685*, 2020.
- [29] Ekin D. Cubuk, Barret Zoph, Jonathon Shlens, and Quoc V. Le. Randaugment: Practical automated data augmentation with a reduced search space, 2019.
- [30] Wei Liu, Dragomir Anguelov, Dumitru Erhan, Christian Szegedy, Scott Reed, Cheng-Yang Fu, and Alexander C Berg. Ssd: Single shot multibox detector. In *European conference on computer vision*, pages 21–37. Springer, 2016.
- [31] Mark Everingham, Luc Van Gool, Christopher KI Williams, John Winn, and Andrew Zisserman. The pascal visual object classes (voc) challenge. *International journal of computer vision*, 88(2):303–338, 2010.
- [32] Tsung-Yi Lin, Michael Maire, Serge Belongie, James Hays, Pietro Perona, Deva Ramanan, Piotr Dollár, and C Lawrence Zitnick. Microsoft coco: Common objects in context. In *European conference on computer vision*, pages 740–755. Springer, 2014.
- [33] Jisoo Jeong, Hyojin Park, and Nojun Kwak. Enhancement of ssd by concatenating feature maps for object detection. In *British Machine Vision Conference*, 2017.
- [34] Cheng-Yang Fu, Wei Liu, Ananth Ranga, Ambrish Tyagi, and Alexander C Berg. Dssd: Deconvolutional single shot detector. *arXiv preprint arXiv:1701.06659*, 2017.